



SERA JRA-6

EMSC

Earthquake Qualitative Impact Assessment

Performance Evaluation

Reviewed by: Alberto Michelini

Submission date: June 14, 2019

Start date of project

1 January 2017

Duration

36 months

Author

S. Julien-Lafferrière

Abstract

EQIA (Earthquake Qualitative Impact Assessment) has been developed by Gilles et al. [1, 2] within the NERIES/JRA-3 project. It provides fast and automatic impact assessment for world crustal earthquakes (depth < 40km) with a magnitude of 5 or higher, in order to quickly detect a potentially damaging earthquake. EQIA does not provide a number of expected fatalities due to too large uncertainties but only a range of possible impact.

EQIA is based on two empirical formulas. The first one proposed by Samardjieva and Badal [3] relates the number of fatalities to the earthquake magnitude and the population density, taken from Land-Scan [4], in the affected area. The second one, suggested by Akkar and Bommer [5] is the GMPE (Ground-Motion Prediction Equation) used to define the impacted area. This document is an analysis of EQIA's performance on 7268 earthquakes (7171 $M < 7$ and 97 $M \geq 7$) from January 2010 to May 2019. EQIA's performance was assessed by comparing EQIA's impact predictions to the NOAA database [6], taken as a reference. The geographical distribution of EQIA's earthquakes in the appendix B summarises these comparisons. EQIA offers excellent performance with more than 98% of correct predictions. However, it is slightly lower when it comes to specifically deadly earthquakes with an 83% success rate. For $M \geq 7$ events, several extreme scenarios are considered to account for the rupture size and propagation. Currently, for $M \geq 7$ events, EQIA provides a right impact in 74% to 83% of the cases depending on the scenario. In the appendix A, the list of all EQIA's incorrect impact predictions is given, Tab. A.1 and A.2.

Most incorrect predictions are for light impact earthquakes since these events are more complex to predict due to being ruled by single events. The only way to tackle this issue would be to have extended and continuous information on the building quality for each region, which is not achievable currently. Some regional biases have been brought to light and will be addressed in the following developments of EQIA along with other improvements that should make EQIA more reliable. Also, additional research leads will be investigated to lower the predictions uncertainties.

Target Audience

This document is intended for all of SERA members, the seismological community and ARISTOLE partners.

Disclaimer

The European Union and its Innovation and Networks Executive Agency (INEA) are not responsible for any use that may be made of the information any communication activity contains.

The content of this publication does not reflect the official opinion of the European Union. Responsibility for the information and views expressed in the therein lies entirely with the author(s).

Contents

List of Figures	4
List of Tables	6
Introduction	7
1 EQIA: a quick description	8
1.1 Method of impact estimate	8
1.1.1 Impact categories	8
1.1.2 Defining the impacted area	9
1.1.3 Population impacted	9
1.1.4 Rupture scenario	9
1.2 Uncertainties integration	11
1.3 Output example	12
2 Performance assessment methodology	15
2.1 Reference data set of impact	15
2.2 Comparison criteria	15
2.3 Aftershocks considerations	16
2.4 Unrealistic ruptures scenarios	16
3 Results and discussions	17
3.1 General results	17
3.1.1 Deadly events	17
3.2 Incorrect predictions	17
3.2.1 Underestimations	19
3.2.2 Overestimation	19
3.3 Region systematic effect	21
3.4 Forthcoming improvements	21
Conclusion	24
A EQIA incorrect estimations	25
B Geographical distribution of EQIA's earthquakes	28
Bibliography	29

List of Figures

1.1	Log–linear regressions based on worldwide data for the number of human victims caused by earthquakes in the 5.0 – 8.0 magnitude interval for different population densities. From [3].	10
1.2	For the April 12th, 2012, M7.0 earthquake in the gulf of California, on the left, the two bilateral scenarios (one for each possible nodal plane), on the right, the past seismicity on the vicinity of the earthquake epicentre. Thanks to this last information the top nodal plane can be considered as non-realistic.	11
1.3	EQIA results for the October 23th, 2011, M7.2 earthquake in eastern Turkey. The displayed scenarios correspond to a bilateral rupture propagation. On the left, a map of the earthquake location with the population density, as well as the modelled rupture (red line) and the iso-PGA boundaries (in black or red). On the right the corresponding impact gauge. 604 fatalities were recorded for this event (heavy impact).	12
1.4	EQIA results for the October 23th, 2011, M7.2 earthquake in eastern Turkey. The displayed scenarios correspond to an unilateral rupture propagation. On the left, a map of the earthquake location with the population density, as well as the modelled rupture (red line) and the iso-PGA boundaries (in black or red). On the right the corresponding impact gauge. 604 fatalities were recorded for this event (heavy impact).	13
1.5	EQIA results for the October 23th, 2011, M7.2 earthquake in eastern Turkey. The displayed scenarios correspond to an unilateral rupture propagation. On the left, a map of the earthquake location with the population density, as well as the modelled rupture (red line) and the iso-PGA boundaries (in black or red). On the right the corresponding impact gauge. 604 fatalities were recorded for this event (heavy impact).	14
3.1	EQIA performance on the 7268 earthquakes (7171 $M < 7$ and 97 $M \geq 7$) and error types when the most favourable case is taken for $M \geq 7$ events.	18
3.2	EQIA performance for the 158 deadly earthquakes when the most favourable scenario is taken for $M \geq 7$ events (the correct rate goes down to 80.4% with the least favourable case).	19
3.3	Impact predicted by EQIA (with uncertainties) compared to the reference impact for the incorrect predictions of EQIA for $M < 7$ events (on the left) and $M \geq 7$ events (on the right).	20
3.4	Geographical distribution of the earthquakes that triggered EQIA from 2004 to 2019 where EQIA overestimates or underestimates the impact. The colour scale corresponds to the difference between the reference impact and the most probable impact predicted by EQIA (< 0 if overestimated and > 0 if underestimated).	21

3.5	Impact predicted by EQIA (with uncertainties) compared to the reference impact for the Mindanao region, Philippines, for the incorrect predictions from 2004 to 2019. The vulnerability changes from "Normal" (on the left) to "Low" (on the right).	22
B.1	Geographical distribution of the earthquakes that triggered EQIA from 2004 to 2019. The colour scale corresponds to the difference between the reference impact and the most probable impact predicted by EQIA (< 0 if overestimated and > 0 if underestimated). Circles are displayed when the reference impact is correctly predicted by EQIA (in range), stars are displayed otherwise (incorrect).	28

List of Tables

1.1	EQIA impact categories.	8
1.2	Regression coefficients for Eq. 1.2 depending on the population density.	10
3.1	Results for 7268 earthquakes (7171 $M < 7$ and 97 $M \geq 7$) from January 2010 to May 2019. For $M \geq 7$ events, the least favourable case is selected.	17
3.2	Results for 7268 earthquakes (7171 $M < 7$ and 97 $M \geq 7$) from January 2010 to May 2019. For $M \geq 7$ events, the most favourable case is selected.	18
3.3	Precedent study results for 719 earthquakes (671 $M < 7$ and 48 $M \geq 7$) before 2010.	18
3.4	Events where EQIA underestimates the earthquake impact, from January 2010 to May 2019.	19
3.5	Events where EQIA overestimates the earthquake impact, from January 2010 to May 2019.	20
A.1	Events where EQIA underestimates the earthquake impact, from January 2010 to May 2019. In green the low impact earthquakes.	25
A.2	Events where EQIA overestimates the earthquake impact, from January 2010 to May 2019. In green the low impact earthquakes.	27

Introduction

As part of the JRA-3 project, the EMSC (European-Mediterranean Seismological Centre) developed a tool capable of rapidly predict human losses due to an earthquake: EQIA (Earthquake Qualitative Impact Assessment). This document is an analysis of EQIA's performance on earthquakes from January 2010 to May 2019.

In the first part of this document, the methodology and equations behind EQIA will be presented. Afterwards, the performance analysis procedure will be explained. Finally, the last part of this report will be dedicated to the results of EQIA's performance assessment and its future improvements.

1 EQIA: a quick description

EQIA (Earthquake Qualitative Impact Assessment) has been developed by Gilles et al. [1, 2] within the NERIES/JRA-3 project. Since 2007, it provides fast and automatic impact assessment for crustal earthquakes (depth < 40km) with a magnitude of 5 or higher. This chapter provides a rapid description of EQIA, for more details, refer to [1, 2].

The purpose of EQIA is to quickly detect a potentially damaging earthquake, depending on its magnitude and on the density of population in the affected region. EQIA does not provide a number of expected fatalities, due to large uncertainties, but only a range of possible impacts.

EQIA has several intrinsic limits. It does not intend to properly estimate the impact of low impact earthquakes where the death toll is controlled by individual accidents. This is for instance the case for the May 1st, 2003, M6.4 earthquake in Bingol, eastern Turkey, which killed over 170 people, 85 whom were killed in the collapse of the dormitory of a primary school.

Likewise, EQIA is rather imprecise concerning moderate magnitudes (from 5 to 6) where the impact zone is comparable to the epicentre location uncertainties. For example, by moving the earthquake epicentre location of the M5.9, September 7th, 1999 in Athens, by 10km, the population impacted by a PGA (Peak Ground Acceleration) over $0.25g$ raises drastically from 1000 to 300000 and the estimated impact from Light to Heavy (see Tab. 1.1).

Furthermore, in the case of an earthquake sequence, it is hard to determine the casualties related to the aftershocks since the population density and the vulnerability may change significantly after the first shock.

1.1 Method of impact estimate

EQIA is mainly based on the empirical formula suggested by Samardjieva and Badal [3] linking the number of casualties to the earthquake magnitude and the population density in the impacted area.

In order to use this formula one has to define the affected area by computing the PGA as a function of magnitude and radius, using the GMPE (Ground-Motion Prediction Equation) from Akkar and Bommer [5].

1.1.1 Impact categories

In view of the large uncertainties, EQIA does not aim to provide an accurate estimate of the number of potential victims. The Tab. 1.1 presents the different impact categories used in EQIA.

Impact category	Fatalities
None	0
Light	1 to 39
Moderate	40 to 99
Heavy	100 to 999
Very Heavy	1000 to 9999
Extreme	> 10000

Table 1.1: EQIA impact categories.

1.1.2 Defining the impacted area

We first consider the PGA evolution as a function of the distance from the epicentre (in km), R , and the magnitude, M , as formulated by Akkar and Bommer [5]:

$$\log_{10}(PGA) = 4.185 - 0.112 \cdot M + (-2.963 + 0.0290 \cdot M) \cdot \log_{10} \left(\sqrt{R^2 + 7.593^2} \right) + 0.099S_S + 0.020S_A - 0.034F_N + 0.104F_R \quad (1.1)$$

Where S_S and S_A are binaries variables taking values of 1 for soft and stiff soil sites and 0 otherwise. F_N and F_R are similarly derived for normal and reverse faulting earthquakes. In our case, rock sites are considered, $S_S = 0$ and $S_A = 1$ and both F_N and F_R are set to 0.

This equation is general and applied to different regions with different type of crustal structures. This is a major hypothesis, it will be addressed in Sec. 3.4.

From 1.1, the iso-PGA boundaries can then be defined by the radius, R :

$$R = \left[10^{2 \cdot \left(\frac{\log_{10}(PGA) - 4.185 + 0.112 \cdot M - 0.020S_A}{-2.963 + 0.0290 \cdot M} \right) - 7.593^2} \right]^{1/2} \quad (1.2)$$

1.1.3 Population impacted

Thanks to the iso-PGA circles defined in the Eq. 1.2, one can determine the area, and therefore the population, impacted by different PGA values. Depending on the region, an empirical parameter is calibrated on past earthquakes: the population vulnerability. The first damages may appear at different PGA thresholds (defined empirically):

- 0.30g for low vulnerability zones (e.g. Japan, Taiwan)
- 0.20g for normal vulnerability zones
- 0.15g for high vulnerability zones (e.g. Afghanistan, Iran)

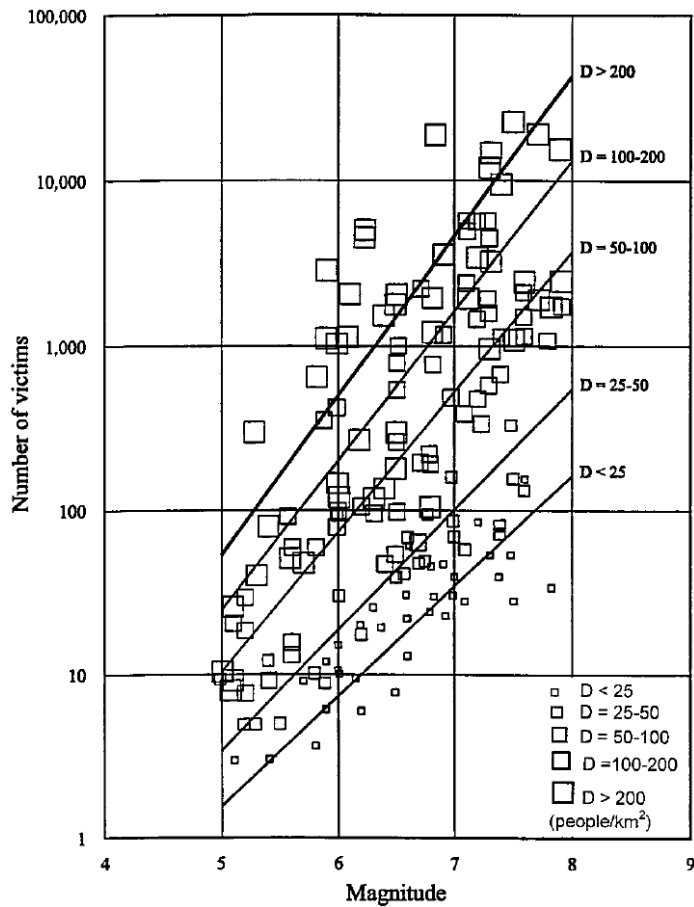
The population data is taken from the LandScan database [4] from the Oak Ridge National Laboratory. Then, the average density, D , is computed and the number of victims, N_V , is obtained from [3]:

$$N_V = 10^{a+b \cdot M} \quad (1.3)$$

Where a and b are depending on D , see Tab. 1.2 and Fig. 1.1.

1.1.4 Rupture scenario

Up to magnitude 7, the rupture is modelled by a point source (0D). For larger magnitudes, $M \geq 7$, the rupture length is no longer negligible. A 1D finite rupture is chosen to model the earthquake rupture (when at least a possible strike angle is know). In this case, the rupture length, L (in km) is computed from the magnitude,



Population density (people/km ²)	<i>a</i>	<i>b</i>
D < 25	-3.41	0.66
D = 25-50	-3.00	0.71
D = 50-100	-2.60	0.75
D = 100-200	-2.17	0.77
D > 200	-2.09	0.86

Table 1.2: Regression coefficients for Eq. 1.2 depending on the population density.

Figure 1.1: Log-linear regressions based on worldwide data for the number of human victims caused by earthquakes in the 5.0 – 8.0 magnitude interval for different population densities. From [3].

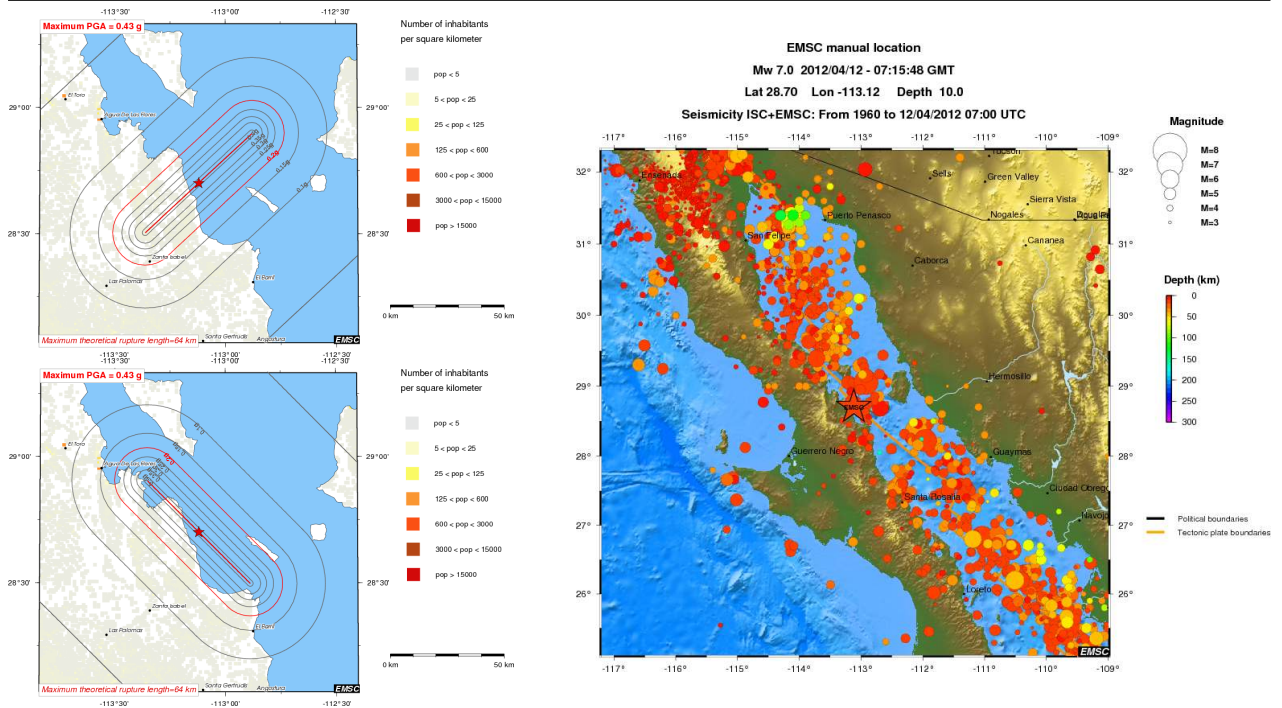


Figure 1.2: For the April 12th, 2012, M7.0 earthquake in the gulf of California, on the left, the two bilateral scenarios (one for each possible nodal plane), on the right, the past seismicity on the vicinity of the earthquake epicentre. Thanks to this last information the top nodal plane can be considered as non-realistic.

M [7]:

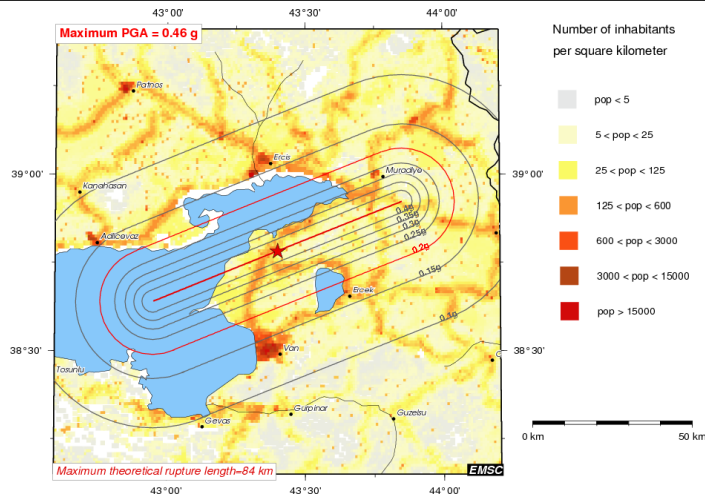
$$\log_{10}(L) = -2.44 + 0.59 \cdot M \quad (1.4)$$

Since we don't have specific information on the rupture propagation, we consider several extreme scenarios. For each nodal plane, obtained from the Global Centroid Moment Tensor (GCMT) database [8, 9], there are 3 endmember scenarios: 2 unilateral ruptures from epicentre and one bilateral. This is envisaged for both nodal planes, bringing the total number of scenarios to 6 for $M \geq 7$ earthquakes. Not all scenarios are as likely, often, one nodal plane (3 scenarios) can be ruled out thanks to the history of the rupture and the tectonic setting, see for example Fig. 1.2.

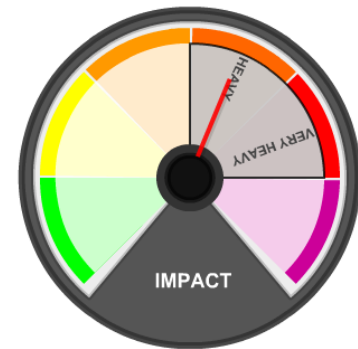
Among the 102 $M \geq 7$ events present in our database, 29 lands scenarios with different impacts. Out of these, 21 can have one nodal plane easily discarded. This will be further developed in Sec. 3.4.

1.2 Uncertainties integration

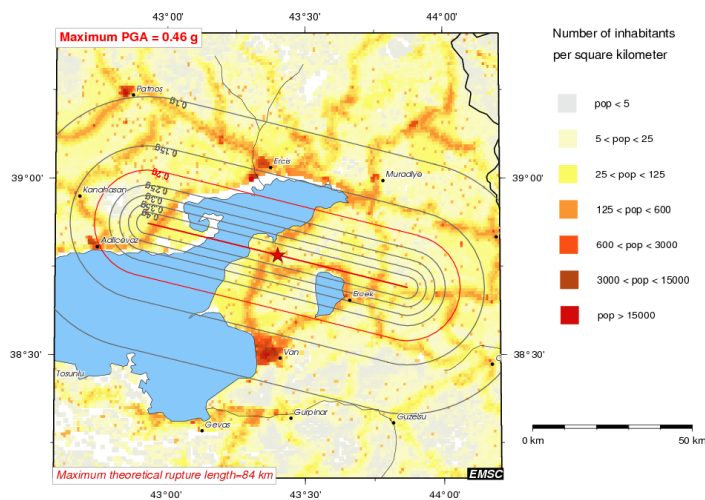
Our knowledge of the magnitude and the location of the epicentre is not perfect. Typical uncertainties are about 0.2 on the magnitude and 15 km on the epicentre location. Depending on the area, this can have a huge impact on the population affected by the earthquake and thus the impact given by EQIA. Thereby, the impact is assessed for a grid of magnitude and location around the epicentre in order to take into account these uncertainties. All the possible outcomes are then analysed to give the probability of each impact.



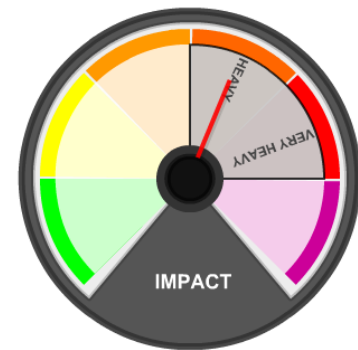
(a) Bilateral rupture scenario, 1st nodal plane.



(b) Associated impact range. The red line points to the most probable impact.



(c) Bilateral rupture scenario, 2nd nodal plane.

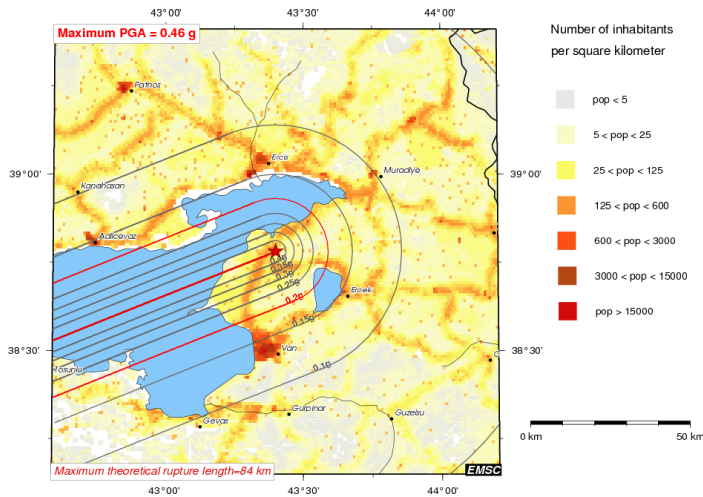


(d) Associated impact range. The red line points to the most probable impact.

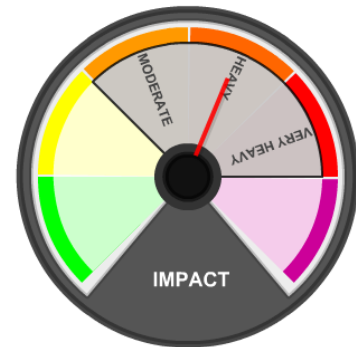
Figure 1.3: EQIA results for the October 23th, 2011, M7.2 earthquake in eastern Turkey. The displayed scenarios correspond to a bilateral rupture propagation. On the left, a map of the earthquake location with the population density, as well as the modelled rupture (red line) and the iso-PGA boundaries (in black or red). On the right the corresponding impact gauge. 604 fatalities were recorded for this event (heavy impact).

1.3 Output example

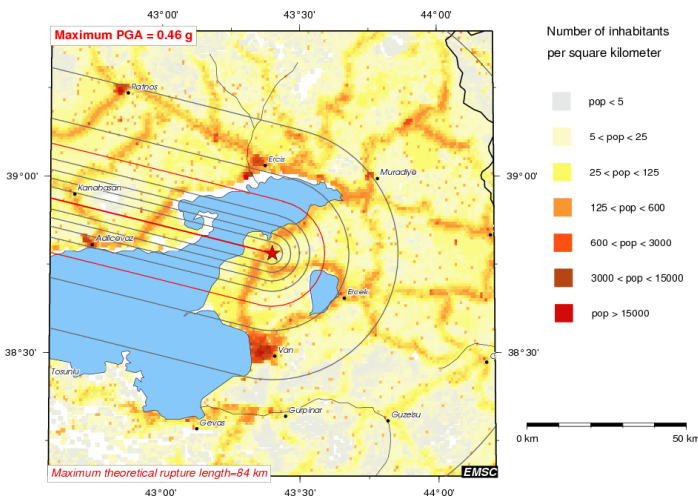
Fig. 1.3, 1.4 and 1.5 show an example of EQIA's results for the October 23th, 2011, M7.2 earthquake in the eastern Turkey. The epicentre location is represented by a red star and the rupture by a red line. The black and red ovals represent the iso-PGA.



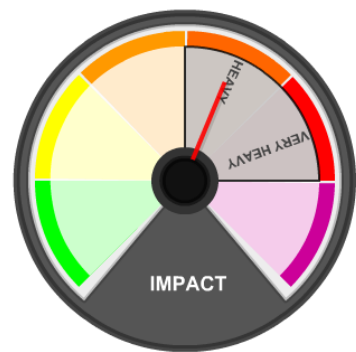
(a) 1st unilateral rupture scenario, 1st nodal plane.



(b) Associated impact range. The red line points to the most probable impact.

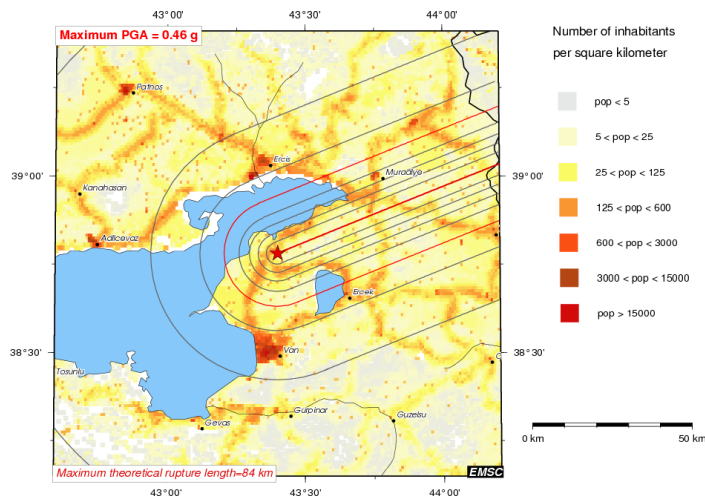


(c) 1st unilateral rupture scenario, 2nd nodal plane.

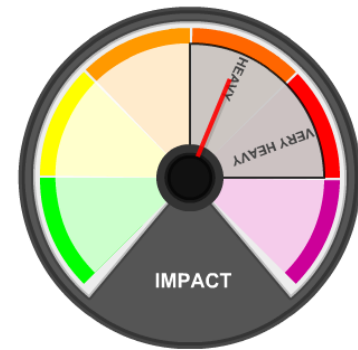


(d) Associated impact range. The red line points to the most probable impact.

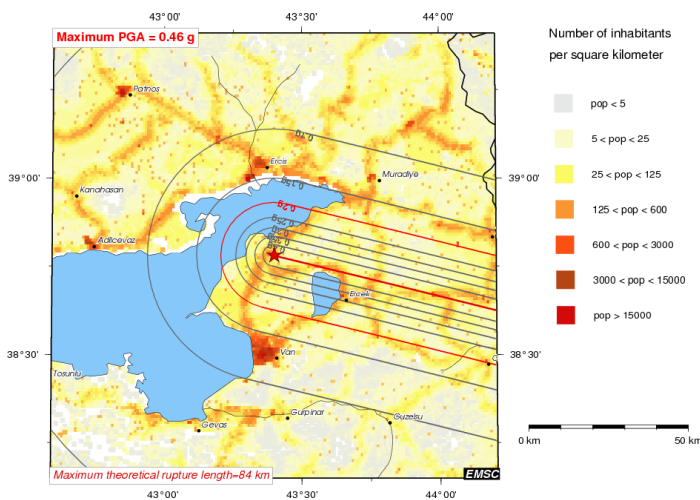
Figure 1.4: EQIA results for the October 23th, 2011, M7.2 earthquake in eastern Turkey. The displayed scenarios correspond to an unilateral rupture propagation. On the left, a map of the earthquake location with the population density, as well as the modelled rupture (red line) and the iso-PGA boundaries (in black or red). On the right the corresponding impact gauge. 604 fatalities were recorded for this event (heavy impact).



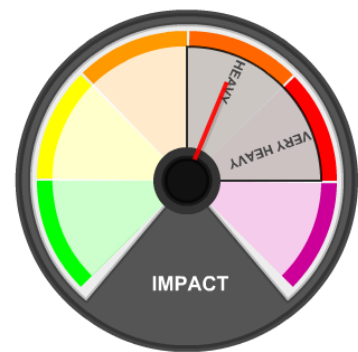
(a) 2nd unilateral rupture scenario, 1st nodal plane.



(b) Associated impact range. The red line points to the most probable impact.



(c) 2nd unilateral rupture scenario, 2nd nodal plane.



(d) Associated impact range. The red line points to the most probable impact.

Figure 1.5: EQIA results for the October 23th, 2011, M7.2 earthquake in eastern Turkey. The displayed scenarios correspond to an unilateral rupture propagation. On the left, a map of the earthquake location with the population density, as well as the modelled rupture (red line) and the iso-PGA boundaries (in black or red). On the right the corresponding impact gauge. 604 fatalities were recorded for this event (heavy impact).

2 Performance assessment methodology

In this part we'll describe the method adopted for the analysis of EQIA's performance. The goal of this analysis is to assess the performance of EQIA by comparing the earthquake impact predicted by EQIA to a reference impact. The analysis focuses on earthquakes from January 2010 (year of the last report [2]) to May 2019. This represents 11457 earthquakes: 11355 $M < 7$ earthquakes and 102 $M \geq 7$ earthquakes.

2.1 Reference data set of impact

The reference impact is taken from the continuously updated NOAA database [6] from the National Centers for Environmental Information (NCEI, formerly the National Geophysical Data Center NGDC), regrouping major earthquakes with a reported number of casualties. We select events from the NOAA database depending on their depth and magnitude to match EQIA scope of application (with a certain uncertainty on magnitude and depth to account for possible discrepancies between NCEI information and ours), for a total of 412 earthquakes. When the number of victims is not indicated, it is expected to be a non-lethal event, thus, the reference impact is "None".

The NOAA earthquakes are associated to EQIA's by comparing the magnitudes, the time of the event and the epicentre location.

2.2 Comparison criteria

Two different comparisons are done:

- In range: the reference impact is between the minimum and the maximum impact predicted by EQIA.
- Exact: the reference impact is the most probable impact predicted by EQIA

In addition, since there are several possible scenarios for $M \geq 7$ earthquakes, as seen in Sec. 1.1.4, we consider two possibilities:

- Most favourable case: when at least one scenario gives a correct impact, the prediction is considered correct.
- Least favourable case: when at least one scenario gives a wrong impact, the prediction is considered incorrect .

When a comparison is incorrect, several categories of errors are distinguished:

- Overestimation: the impact predicted by EQIA is higher than the reference impact.
- Positive fake: the impact predicted by EQIA is higher than the reference impact which is "None" (particular case of the overestimation category).
- Underestimation: the impact predicted by EQIA is lower than the reference impact.
- Negative fake: the impact predicted by EQIA is "None" and is lower than the reference impact (particular case of the underestimation category).

- Uncategorisable: for events with scenarios leading to different impacts higher or lower than the reference impact.

2.3 Aftershocks considerations

It is difficult to discern the human losses associated with an aftershock in relation to the main earthquake (main shock). In addition, various biases affect the quality of the estimate of the number of victims: the most fragile buildings are already destroyed, the population is more vigilant, a part of the population may have been evacuated, etc. In order to avoid biases, the aftershocks are removed from the analysis by roughly grouping them into clusters (without taking into account possible fore shocks) using time-space correlations. For each cluster only the main shock is analysed. From the initial 11457 earthquakes, 4189 are pulled out of the analysis (4184 $M < 7$ and 5 $M \geq 7$).

Remark: An aftershock could have a main shock with a depth possibly above 40km, which won't be present in EQIA. Due to this limit, some aftershocks might not be ruled out.

2.4 Unrealistic ruptures scenarios

As we discussed in Sec. 1.1.4, several rupture scenarios are tested for $M \geq 7$ events. In some cases, one of the nodal planes can be discarded thanks to our knowledge of tectonic. In order to avoid biases, the scenarios associated with such nodal planes are not analysed.

3 Results and discussions

In this last chapter, the results of the comparison between NOAA and EQIA are detailed and the impending improvements are presented.

3.1 General results

The following tables summarise the results for the most and least favourable cases, respectively Tab. 3.1 and 3.2, for the two types of comparison (In range and Exact).

In overall, EQIA presents very good performance and is able to correctly predict the impact of the vast majority of earthquakes. However, the performance of EQIA for major earthquakes ($M \geq 7$), while being very satisfactory, is well below the general performance, in particular for the "Exact" case since the uncertainties for $M \geq 7$ events are strongly impacting the output. For $M \geq 7$ events, EQIA's performance lies between the most and least favourable cases; since several scenarios are analysed for one earthquake. In order to manage ideally an $M \geq 7$ event, only one scenario shall remain, this point will be further discussed in Sec. 3.4

A detailed version of the results for the most favourable case is displayed in Fig. 3.1. For the vast majority of events, the impact range given by EQIA includes the reference impact and most of the errors are positive fakes.

This analysis can be compared to the previous study [2], summarised in Tab. 3.3, which shows similar results considering the lesser statistic.

3.1.1 Deadly events

If we now consider only the deadly earthquakes, the performance of EQIA is presented in Fig. 3.2.

Even though it is lower than the overall performance, it is still enough when acknowledging the major sources of uncertainties.

3.2 Incorrect predictions

The impact predicted by EQIA compared to the reference impact for incorrect predictions are displayed in Fig. 3.3. Most of these errors are overestimations (positive fakes): EQIA predicts a "Light" or "Moderate" impact where the earthquake didn't make any reported victim (impact "None").

As we said before, light impact earthquakes are particularly tricky to address, a local very vulnerable zone

Result (least favourable case)	All		M<7		M≥7	
	In range	Exact	In range	Exact	In range	Exact
Correct	98.6%	92.5%	98.9%	92.9%	74.5%	61.2%
Overestimation	1.0%	6.6%	0.8%	6.3%	15.3%	26.5%
Underestimation	0.2%	0.7%	0.2%	0.7%	2.0%	2.0%
Uncategorisable	0.1%	0.1%	-	-	8.2%	10.2%

Table 3.1: Results for 7268 earthquakes (7171 $M < 7$ and 97 $M \geq 7$) from January 2010 to May 2019. For $M \geq 7$ events, the least favourable case is selected.

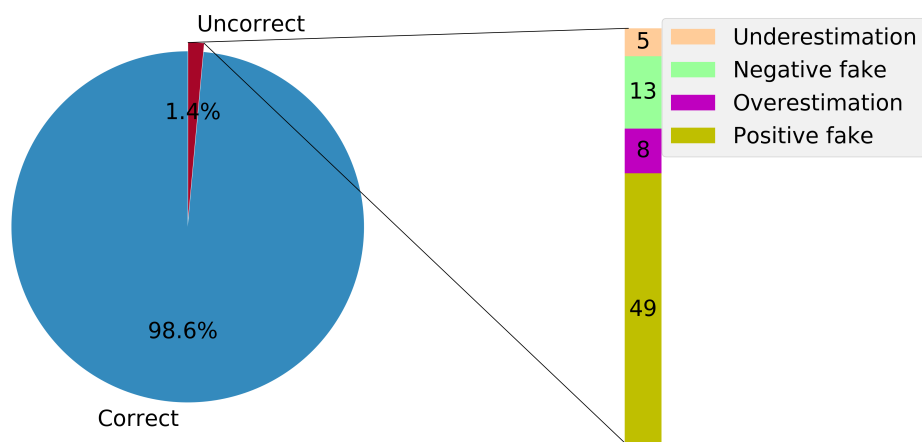


Figure 3.1: EQIA performance on the 7268 earthquakes (7171 $M < 7$ and 97 $M \geq 7$) and error types when the most favourable case is taken for $M \geq 7$ events.

Result (most favourable case)	All		$M < 7$		$M \geq 7$	
	In range	Exact	In range	Exact	In range	Exact
Correct	98.7%	92.6%	98.9%	92.9%	82.7%	68.4%
Overestimation	1.0%	6.6%	0.8%	6.3%	15.3%	26.5%
Underestimation	0.2%	0.7%	0.2%	0.7%	2.0%	2.0%
Uncategorisable	0.0%	0.0%	-	-	0.0%	3.1%

Table 3.2: Results for 7268 earthquakes (7171 $M < 7$ and 97 $M \geq 7$) from January 2010 to May 2019. For $M \geq 7$ events, the most favourable case is selected.

Result	$M < 7$ In range	$M \geq 7$	
		(favourable case) In range	(unfavourable case) In range
Correct	96%	88%	68%
Overestimation	2%	8%	17%
Underestimation	2%	4%	15%

Table 3.3: Precedent study results for 719 earthquakes (671 $M < 7$ and 48 $M \geq 7$) before 2010.

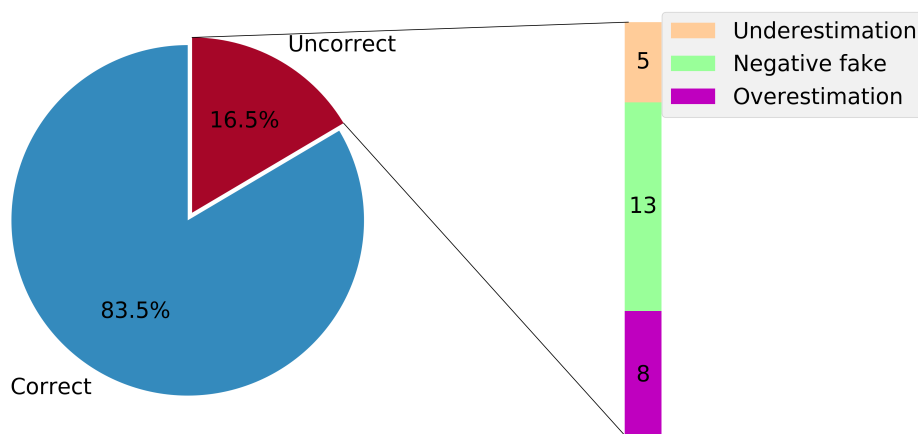


Figure 3.2: EQIA performance for the 158 deadly earthquakes when the most favourable scenario is taken for $M \geq 7$ events (the correct rate goes down to 80.4% with the least favourable case).

Date	Region	Lat, Lon	Mag.	Ref. impact	EQIA impact
13/04/2010	Southern Qinghai, China	33.2, 96.7	6.9	Very Heavy	Light
18/09/2011	Sikkim, India	27.8, 88.2	6.9	Heavy	None to Light
11/06/2012	Hindu Kush region, Afghanistan	36.1, 69.4	5.7	Moderate	None to Light
02/07/2013	Northern Sumatra, Indonesia	4.7, 96.6	6.1	Moderate	None to Light
24/08/2016	Central Italy	42.7, 13.2	6.2	Heavy	None to Light
28/09/2018	Minahasa, Sulawesi, Indonesia	-0.2, 119.9	7.5	Very Heavy	Mod. to Heavy

Table 3.4: Events where EQIA underestimates the earthquake impact, from January 2010 to May 2019.

(e.g.: dilapidated apartment block) can cause severe casualties even for low impact earthquakes.

3.2.1 Underestimations

The worst error EQIA can do is underestimate a moderate to extreme impact event (as we discussed, light impact earthquakes can't be well estimated).

Tab. A.1, appendix A, gives the details of all the underestimations. As it can be seen, most of them are light impact earthquakes (14 out of 20). If these are discarded, 6 cases remain where EQIA gives, in a problematic way, a lower impact than the reference, Tab. 3.4. Among these, the August 28th, 2018, Minahasa earthquake is a particular case since it caused a tsunami (EQIA is not meant to predict tsunami casualties). The reported fatalities are due to the earthquake and the following tsunami, it is very difficult to disentangle the two.

3.2.2 Overestimation

If we follow the same path for the overestimations, from Tab. A.2 in appendix A, we can select the relevant events, Tab. 3.5. EQIA tends to, proportionally, overestimate especially $M \geq 7$ events.

As one can see from Tab. 3.4 and 3.5, only a few events put truly EQIA in default. EQIA turns out to be a very reliable tool to predict the impact of an earthquake.

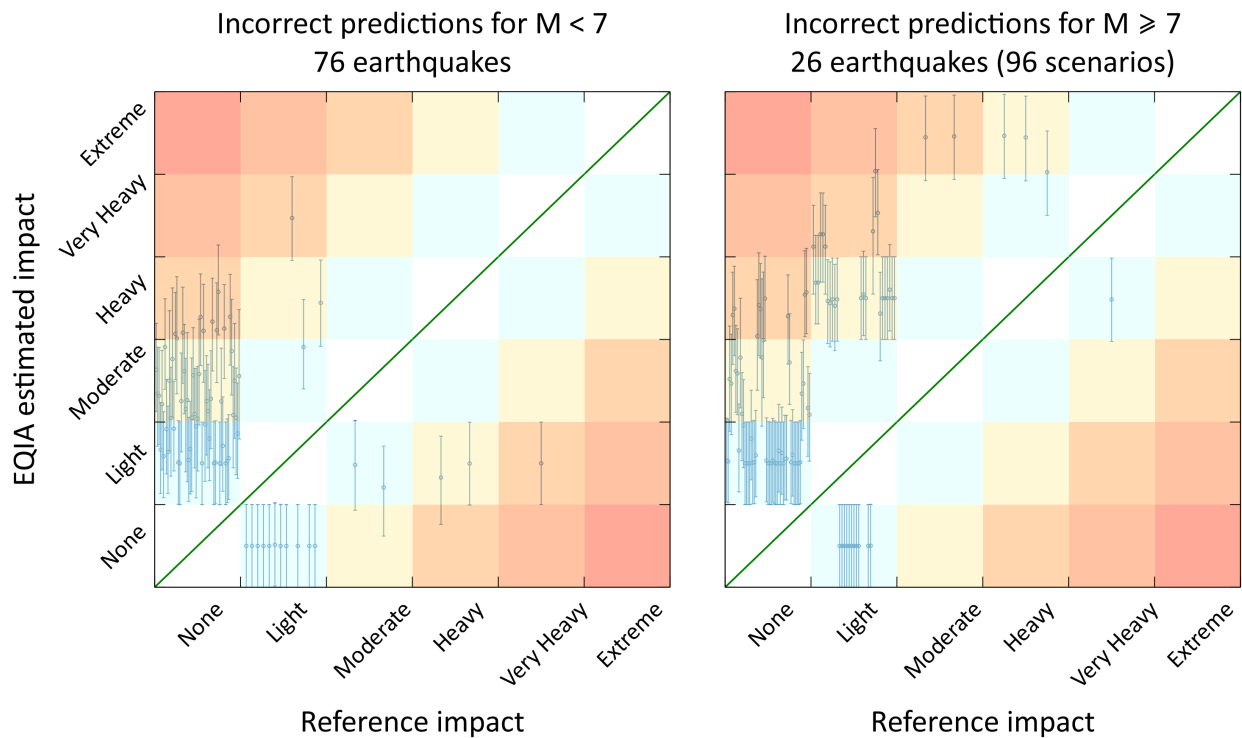


Figure 3.3: Impact predicted by EQIA (with uncertainties) compared to the reference impact for the incorrect predictions of EQIA for $M < 7$ events (on the left) and $M \geq 7$ events (on the right).

Date	Region	Lat, Lon	Mag.	Ref. impact	EQIA impact
30/01/2010	Eastern Sichuan, China	30.3, 105.8	5.3	None	Mod. to Heavy
06/04/2010	Northern Sumatra, Indonesia	2.3, 97.1	7.7	None	Mod. to Heavy
20/03/2012	Guerrero, Mexico	16.7, -98.2	7.4	Light	Heavy to V. Heavy
25/03/2012	Maule, Chile	-35.2, -72.1	7.1	Light	Mod. to Heavy
05/09/2012	Costa Rica	10.2, -85.4	7.6	Light	Heavy
15/10/2013	Bohol, Philippines	9.9, 124.1	7.1	Heavy	V. Heavy to Extr.
28/06/2015	Assam, India	26.6, 90.5	5.5	None	Mod. to Heavy
16/09/2015	Offshore Coquimbo, Chile	-31.6, -71.6	8.3	Light	Heavy to Extr.
12/02/2016	Sumba, Indonesia	-9.6, 119.5	6.3	None	Light to V. Heavy
15/04/2016	Kyushu, Japan	32.8, 130.7	7	Mod.	V. Heavy to Extr.
13/11/2016	South island of New Zealand	-42.7, 173.0	7.9	Light	Mod. to Heavy
16/02/2018	Oaxaca, Mexico	16.6, -97.7	7.2	Light	Heavy to V. Heavy
05/08/2018	Lombok, Indonesia	-8.3, 116.5	7	Heavy	V. Heavy to Extr.
12/09/2018	Assam, India	26.4, 90.4	5.3	Light	Mod. to Heavy
22/04/2019	Luzon, Philippines	14.9, 120.5	6.1	Light	Heavy

Table 3.5: Events where EQIA overestimates the earthquake impact, from January 2010 to May 2019.

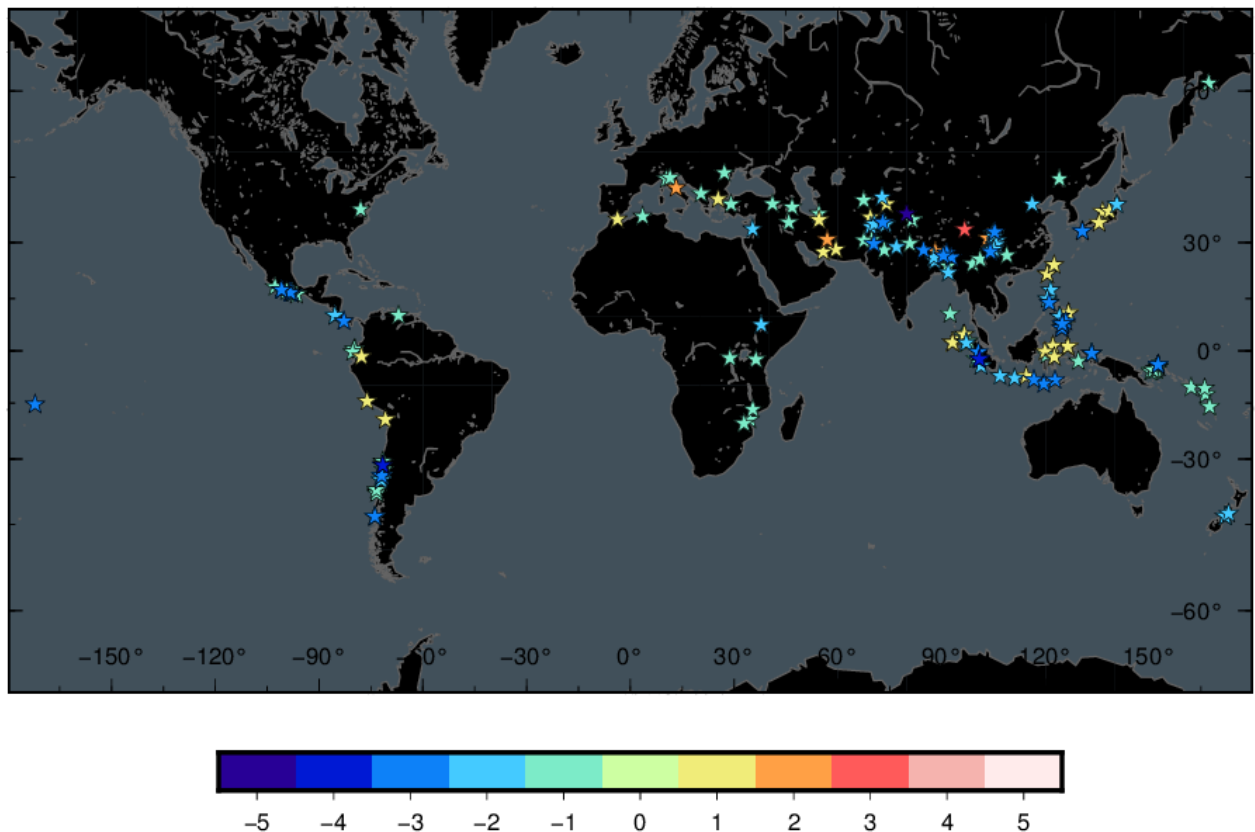


Figure 3.4: Geographical distribution of the earthquakes that triggered EQIA from 2004 to 2019 where EQIA overestimates or underestimates the impact. The colour scale corresponds to the difference between the reference impact and the most probable impact predicted by EQIA (< 0 if overestimated and > 0 if underestimated).

3.3 Region systematic effect

One can wonder if there is any regional systematic effect, due in particular to the GMPE used, see Sec. 1.1. In order to identify a recurrent overestimation or underestimation of the earthquakes impact in a specific region, the earthquakes from 2004 to 2019 are analysed (in order to increase statistics). The Fig. 3.4 represents the geographical distribution of EQIA's incorrect predictions. As a comparison, Fig. B.1, in the appendix B, displays all the results (correct and incorrect impact estimations).

The Mindanao region, Philippines, is over-represented on this map. It is an example of a systematic regional effect. There are two solutions to tackle this issue. As a first order correction, the region vulnerability could be changed. This is illustrated in Fig. 3.5, where the same computation has been done for several earthquakes in the Mindanao region with a change on the vulnerability parameter. It has a drastic impact on the quality of the predictions: almost all the events are well estimated after the vulnerability change.

The second solution is more satisfying and is part of the foreseen improvements for EQIA.

3.4 Forthcoming improvements

This section sums up all the planned improvements for EQIA.

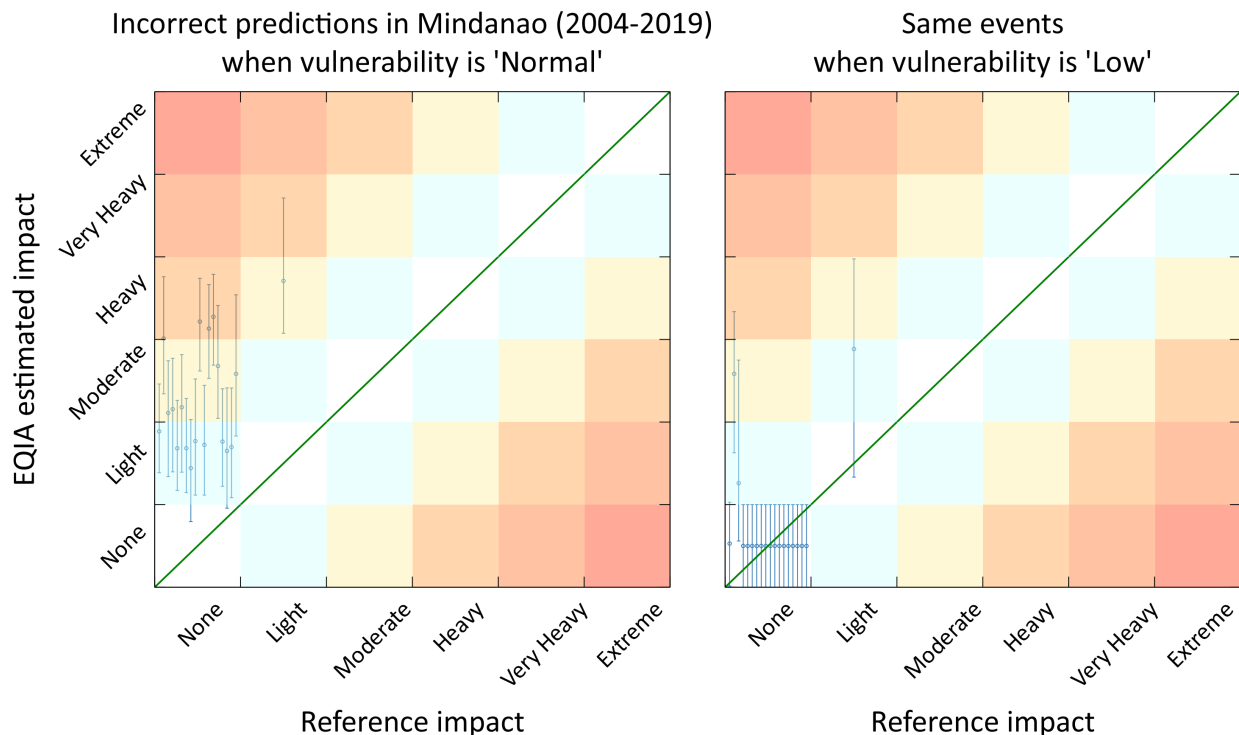


Figure 3.5: Impact predicted by EQIA (with uncertainties) compared to the reference impact for the Mindanao region, Philippines, for the incorrect predictions from 2004 to 2019. The vulnerability changes from "Normal" (on the left) to "Low" (on the right).

Low to medium depth earthquake: we want to extend the scope of EQIA to low and moderate depth mantle earthquakes (depth < 200km), involving dedicated GMPE.

Region specific GMPE: the upcoming GFZ Ground Motion Predictive Equations web service [10] will allow to replace Eq. 1.1 by a region determined equation. Such improvements along with the resulting vulnerability calibration shall remove most systematic effects such as the one seen in the Mindanao region and reduce the number of incorrect predictions (Tab. 3.4 and Tab. 3.5).

Lowering uncertainties: in order to reduce the uncertainties on the EQIA predictions, EQIA will be launched 20 minutes after the earthquake, when the magnitude is better constrained. Indeed, in the EMSC database, over 85% of the earthquakes magnitude are defined within 0.1 of their final magnitude 20 minutes after they occurred. This will also avoid multiple launches of EQIA when the magnitude is reappraised in the first 20 minutes (if the magnitude is reassessed after 20 minutes, EQIA will still update its results accordingly).

Also, when a reliable institute close to the earthquake site provides us with the epicentre location, it's expected to be precise enough to lower the uncertainties from the current 15km to 10km.

Population density information: EQIA will be moving from LandScan to the Global Human Settlement Population Grid [11], provided by the European Commission. It has the advantage of having a better spatial resolution (250m or 1km).

Rupture length: Eq. 1.4 might be update with more recent and comprehensive work on rupture length [12, 13].

Bathymetry and topography: as we have seen in Sec. 2.4, it is mandatory to know the correct scenario for $M \geq 7$ ruptures. In order to select the legitimate scenario with the maximum information, several decision support mechanisms will be implemented. The topography and bathymetry of the area along the epicentre will be added to the output maps to facilitate the choice of the most probable nodal plane.

Felt reports integration: for some $M \geq 7$ events, the bathymetry and topography are not enough to safely exclude one rupture orientation.

By merging it with other information gathered by the CSEM (visitors on the website, felt reports collected by the EMSC LastQuake App), we can expect to be able to exclude every time one nodal plane and in the best case have only one rupture scenario left.

Conclusion

EQIA's performance has been assessed by comparing EQIA's impact predictions to a reference. EQIA presents excellent performance with more than 98% of correct predictions and 82% for $M \geq 7$ in the most favourable scenario. When it comes to specifically deadly earthquakes, EQIA remains accurate with an 83% success rate in the most favourable scenario.

Most failures are for light impact earthquakes since these events are more complex to predict due to being ruled by single events. The only way to tackle this issue would be to have extended and continuous information on the building quality for each region, which is not achievable currently.

Some regional biases have been brought to light and will be addressed in the following developments of EQIA along with other improvements that should make EQIA more reliable and precise.

A EQIA incorrect estimations

The tables below regroup all the failed estimation from January 2010 to May 2019, for the underestimations, Tab. A.1 and the overestimations, Tab. A.2.

Date	Region	Lat, Lon	Mag.	Ref. impact	EQIA impact
13/04/2010	Southern Qinghai, China	33.2, 96.7	6.9	V. Heavy	Light
27/08/2010	Northern Iran	35.5, 54.6	5.7	Light	None
18/09/2011	Sikkim, India	27.8, 88.2	6.9	Heavy	None to Light
28/10/2011	Near coast of Central Peru	-14.5, -76.1	6.9	Light	None
11/04/2012	Off west coast of Northern Sumatra	2.4, 93.2	8.4	Light	None
11/06/2012	Hindu Kush Reg., Afghanistan	36.1, 69.4	5.7	Mod.	None to Light
31/08/2012	Philippine islands Reg.	10.9, 126.7	7.6	Light	None
02/07/2013	Northern Sumatra, Indonesia	4.7, 96.6	6.1	Mod.	None to Light
01/04/2014	Offshore Tarapaca, Chile	-19.7, -70.9	8.1	Light	None
24/05/2014	Aegean sea	40.3, 25.4	6.9	Light	None
20/04/2015	Taiwan Reg.	24.2, 122.5	6.4	Light	None
25/01/2016	Strait of Gibraltar	35.7, -3.7	6.3	Light	None
24/08/2016	Central Italy	42.7, 13.2	6.2	Heavy	None to Light
25/11/2016	Southern Xinjiang, China	39.2, 74.0	6.6	Light	None
31/01/2018	Ecuador	-1.7, -77.8	5.2	Light	None
17/06/2018	Near south coast of Western Honshu	34.8, 135.5	5.6	Light	None
07/09/2018	Southeastern Iran	28.3, 59.4	5.5	Light	None
28/09/2018	Minahasa, Sulawesi, Indonesia	-0.2, 119.9	7.5	V. Heavy	Mod. to Heavy
10/10/2018	Bali sea	-7.4, 114.4	6	Light	None
12/04/2019	Sulawesi, Indonesia	-1.8, 122.6	6.8	Light	None

Table A.1: Events where EQIA underestimates the earthquake impact, from January 2010 to May 2019. In green the low impact earthquakes.

Date	Region	Lat, Lon	Mag.	Ref. impact	EQIA impact
30/01/2010	Eastern Sichuan, China	30.3, 105.8	5.3	None	Mod. to Heavy
09/02/2010	Oaxaca, Mexico	16.1, -96.6	5.6	None	Light to Mod.
11/03/2010	Libertador O'Higgins, Chile	-34.2, -71.9	7.2	None	Light to Heavy
06/04/2010	Northern Sumatra, Indonesia	2.3, 97.1	7.7	None	Mod. to Heavy
26/06/2010	Rajasthan, India	28.1, 73.4	5.4	None	Light to Heavy
14/07/2010	Bio-Bio, Chile	-37.9, -73.3	6.6	None	Light to Heavy
18/07/2010	New Britain Reg., P.N.G.	-6.1, 150.5	7.1	None	Light
03/09/2010	South island of New Zealand	-43.3, 172	7	None	Light to Heavy
10/09/2010	Sichuan-Chongqing Bdr. Reg., China	29.5, 105.6	5	None	Light to Mod.
15/11/2010	Hindu Kush Reg., Afghanistan	34.5, 70.5	5.2	None	Light to Heavy
19/12/2010	Ethiopia	7.5, 37.8	5.2	None	Light to Heavy
02/01/2011	Bio-Bio, Chile	-38.3, -73.4	7.1	None	Light
04/04/2011	Nepal-India Bdr. Reg.	29.8, 80.8	5.6	None	Light to Heavy
19/05/2011	Western Turkey	39.2, 29.1	5.8	None	Light to Heavy
23/08/2011	Virginia	38, -78	5.8	None	Light to Mod.
31/10/2011	Sichuan-Gansu Bdr. Reg., China	32.6, 105.3	5.7	None	Light to Heavy
05/03/2012	Haryana-Delhi Reg., India	28.9, 77	5.2	None	Light to Heavy
08/03/2012	Mindoro, Philippines	13.8, 121.1	5.4	None	Light to Heavy
20/03/2012	Guerrero, Mexico	16.7, -98.2	7.4	Light	Heavy to V. Heavy
25/03/2012	Maule, Chile	-35.2, -72.1	7.1	Light	Mod. to Heavy
27/03/2012	Nepal-India Bdr. Reg.	26.2, 87.8	5	None	Light to Mod.
11/04/2012	Michoacan, Mexico	18.3, -102.7	6.7	None	Light
11/05/2012	Assam, India	26.2, 92.8	5.4	None	Light to Heavy
20/05/2012	Northern Italy	44.8, 11.4	5.2	None	Light to Mod.
11/08/2012	Northwestern Iran	38.5, 46.8	6.3	None	Light to Mod.
03/09/2012	Mindanao, Philippines	8.0, 125.2	5.6	None	Light to Heavy
05/09/2012	Costa Rica	10.2, -85.4	7.6	Light	Heavy
07/09/2012	Sichuan-Yunnan-Guizhou Reg., China	27.7, 104.1	5.6	None	Light to Heavy
08/02/2013	Santa Cruz islands	-10.8, 166.1	7	None	Light to Mod.
24/04/2013	Eastern Sichuan, China	28.5, 105.0	5.2	None	Light to Heavy
26/05/2013	Eastern Uzbekistan	40.0, 67.4	5.8	None	Light to Heavy
01/06/2013	Mindanao, Philippines	7.3, 124.9	5.6	None	Light to Heavy
21/08/2013	Guerrero, Mexico	17.1, -99.3	6.2	None	Light to Heavy
29/09/2013	Bio-Bio, Chile	-37.4, -73.4	5.6	None	Light to Mod.
15/10/2013	Bohol, Philippines	9.9, 124.1	7.1	Heavy	V. Heavy to Extr.
22/11/2013	Jilin, China	44.6, 124.0	5.4	None	Light to Mod.
18/04/2014	Guerrero, Mexico	17.5, -100.9	7.2	None	Light to Heavy
29/07/2014	Eastern Sichuan, China	31.6, 105.1	5	None	Light to Mod.
23/08/2014	Valparaiso, Chile	-32.6, -71.3	6.4	None	Light to Heavy
22/11/2014	Romania	45.9, 27.2	5.6	None	Light to Heavy
26/02/2015	Pakistan	34.7, 73.3	5.3	None	Light to Heavy

Date	Region	Lat, Lon	Mag.	Ref. impact	EQIA impact
29/03/2015	New Britain, P.N.G.	-4.8, 152.6	7.5	None	Light
30/03/2015	Guizhou, China	26.7, 108.9	5.4	None	Light to Heavy
05/05/2015	New Britain, P.N.G.	-5.5, 152.0	7.4	None	Light
28/06/2015	Assam, India	26.6, 90.5	5.5	None	Mod. to Heavy
02/07/2015	Pakistan	34.4, 73.8	5.3	None	Light to Heavy
07/08/2015	Lac Kivu , Congo	-2.2, 28.8	5.5	None	Light to Heavy
16/09/2015	Offshore Coquimbo, Chile	-31.6, -71.6	8.3	Light	Heavy to Extr.
23/10/2015	Pakistan	29.6, 70.4	5.5	None	Light to Heavy
07/11/2015	Coquimbo, Chile	-30.9, -71.5	6.9	None	Light
10/02/2016	Coquimbo, Chile	-30.6, -71.6	6.3	None	Light
12/02/2016	Sumba, Indonesia	-9.6, 119.5	6.3	None	Light to V. Heavy
21/02/2016	Nepal	28.1, 84.8	5.5	None	Light to Heavy
15/04/2016	Kyushu, Japan	32.8, 130.7	7	Mod.	V. Heavy to Extr.
28/04/2016	Vanuatu	-16.0, 167.5	7	None	Light to Mod.
18/05/2016	Near coast of Ecuador	0.5, -79.8	6.7	None	Light
28/05/2016	Northern Algeria	36.4, 3.5	5.2	None	Light to Mod.
11/07/2016	Near coast of Ecuador	0.6, -79.7	6.3	None	Light
04/09/2016	Mindanao, Philippines	8.4, 125.9	5.7	None	Light to Heavy
13/11/2016	South island of New Zealand	-42.7, 173.0	7.9	Light	Mod. to Heavy
25/12/2016	Isla Chiloe, Los Lagos, Chile	-43.4, -73.9	7.6	None	Light
27/12/2016	Sichuan-Chongqing Bdr. Reg., China	29.5, 105.8	5	None	Light to Mod.
18/01/2017	Eastern Sichuan, China	28.2, 104.9	5	None	Light to Mod.
27/01/2017	Eastern Sichuan, China	28.2, 104.9	5.3	None	Light to Heavy
11/04/2017	Mindanao, Philippines	7.7, 124.9	5.8	None	Light to Heavy
29/05/2017	Sulawesi, Indonesia	-1.3, 120.4	6.6	None	Light to Heavy
24/06/2017	Mozambique	-19.6, 34.5	5.6	None	Light to Heavy
23/09/2017	Mindanao, Philippines	7.7, 124.9	5.7	None	Light to Heavy
30/09/2017	Sichuan-Gansu Bdr. Reg., China	32.3, 105	5.4	None	Light to Mod.
03/12/2017	Near coast of Ecuador	-0.39, -80.3	6	None	Light
11/12/2017	Iran-Iraq Bdr. Reg.	34.9, 45.8	5.4	None	Light
16/02/2018	Oaxaca, Mexico	16.6, -97.7	7.2	Light	Heavy to V. Heavy
08/03/2018	Mozambique	-16.8, 35.4	5.5	None	Light to Heavy
05/08/2018	Lombok , Indonesia	-8.3, 116.5	7	Heavy	V. Heavy to Extr.
12/09/2018	Assam, India	26.4, 90.4	5.3	Light	Mod. to Heavy
10/10/2018	New Britain, P.N.G.	-5.6, 151.2	7	None	Light to Mod.
16/12/2018	Sichuan-Guizhou Bdr. Reg., China	28.3, 105.1	5.4	None	Light to Heavy
22/12/2018	Mozambique	-20.7, 32.8	5.5	None	Light to Heavy
22/04/2019	Luzon, Philippines	14.9, 120.5	6.1	Light	Heavy
12/05/2019	Panama-Costa Rica Bdr. Reg.	8.6, -82.8	6.1	None	Light to Heavy
14/05/2019	New Britain, P.N.G.	-4.08, 152.6	7.5	None	Light to Mod.

Table A.2: Events where EQIA overestimates the earthquake impact, from January 2010 to May 2019. In green the low impact earthquakes.

B Geographical distribution of EQIA's earthquakes

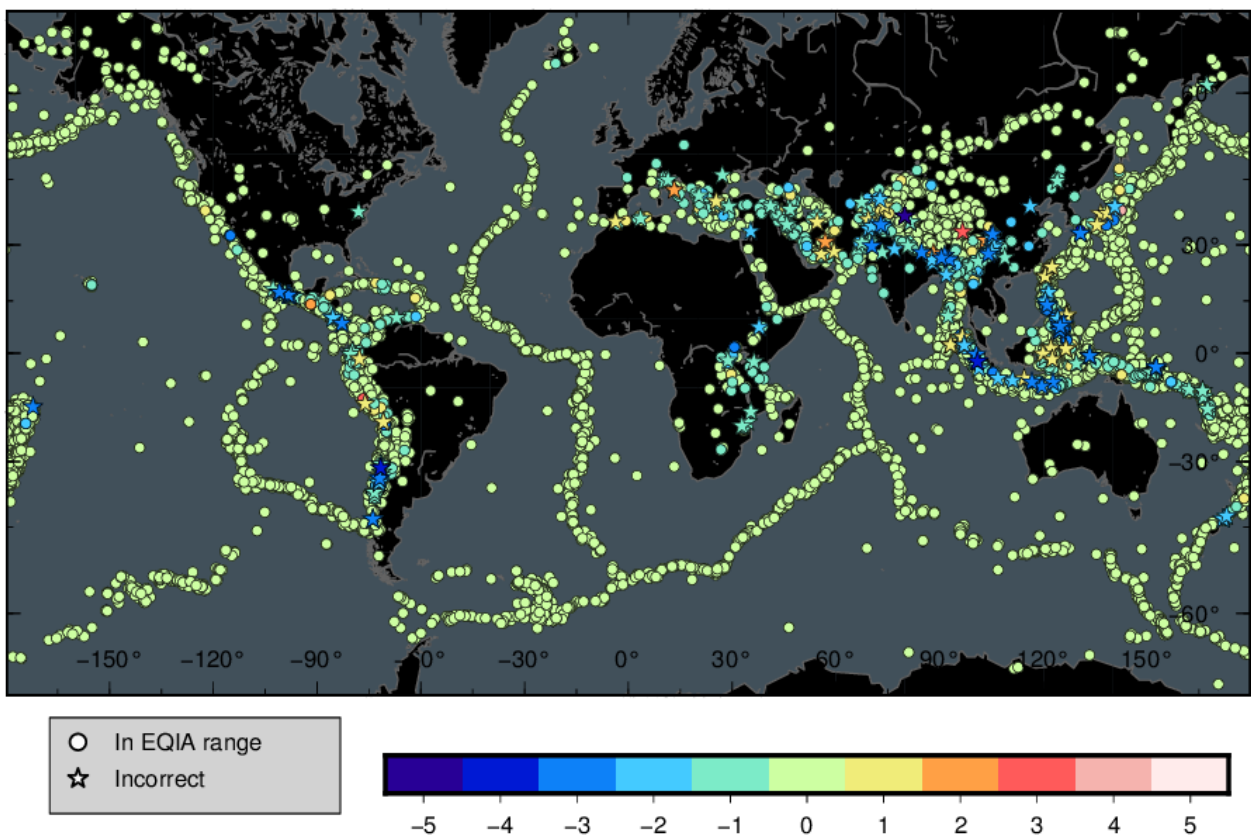


Figure B.1: Geographical distribution of the earthquakes that triggered EQIA from 2004 to 2019. The colour scale corresponds to the difference between the reference impact and the most probable impact predicted by EQIA (< 0 if overestimated and > 0 if underestimated). Circles are displayed when the reference impact is correctly predicted by EQIA (in range), stars are displayed otherwise (incorrect).

Bibliography

- [1] J. Roger et al., “Applications and Utilization of ELER Software,” *NERIES JRA3-D5*, 2009.
- [2] S. Gilles et al., “Utilization of ELER V2 and Improvement of EMSC Earthquake Impact Estimation Method,” *NERIES JRA3-D5*, 2010.
- [3] E. Samardjieva and J. Badal, “Estimation of the Expected Number of Casualties Caused by Strong Earthquakes,” *B. Seismol. Soc. Am.*, vol. 92, no. 6, pp. 2310–2322, 2002.
- [4] Oak Ridge National Laboratory, “LandScan™ High Resolution global Population Data Set copyrighted by UT-Battelle, LLC, operator of Oak Ridge National Laboratory under Contract No. DE-AC05-00OR22725 with the United States Department of Energy,” accessed on May 2019. <https://landscan.ornl.gov>.
- [5] S. Akkar and J. J. Bommer, “Prediction of elastic displacement response spectra in Europe and the Middle East,” *Earthquake Engng Struct. Dyn.*, vol. 36, pp. 1275–1301, 2007.
- [6] National Centers for Environmental Information, accessed on May 2019. <https://www.ngdc.noaa.gov/hazard>.
- [7] D. L. Wells and K. J. Coppersmith, “New Empirical Relationships among Magnitude, Rupture Length, Rupture Width, Rupture Area, and Surface Displacement,” *B. Seismol. Soc. Am.*, vol. 84, no. 4, pp. 974–1002, 1994.
- [8] A. M. Dziewonski, T.-A. Chou and J. H. Woodhouse, “Determination of earthquake source parameters from waveform data for studies of global and regional seismicity,” *J. Geophys. Res.*, vol. 86, pp. 2825–2852, 1981.
- [9] G. Ekström, M. Nettles, and A. M. Dziewonski, “The global CMT project 2004-2010: Centroid-moment tensors for 13,017 earthquakes,” *Phys. Earth Planet. Inter.*, vol. 200-201, pp. 1–9, 2012.
- [10] GFZ Helmholtz Centre Potsdam, German Research Centre for Geosciences, accessed on May 2019. <https://www.gfz-potsdam.de/en/research/data-products-services/>.
- [11] S. Freire et al., “Development of new open and free multi-temporal global population grids at 250 m resolution,” *AGILE 2016*, 2016.
- [12] M. Leonard, “Earthquake Fault Scaling: Self-Consistent Relating of Rupture Length, Width, Average Displacement, and Moment Release,” *B. Seismol. Soc. Am.*, vol. 100, no. 5, pp. 1971–1988, 2010.
- [13] M. Leonard, “Self-Consistent Earthquake Fault-Scaling Relations; Update and Extension to Stable Continental Strike-Slip Faults,” *B. Seismol. Soc. Am.*, vol. 104, no. 6, pp. 2953–2965, 2014.